Research Article

Received: 9 March 2019 Revised: 2 April 2019 Accepted article published: 10 April 2019 Published online in Wiley Online Library: 29 April 2019

(wileyonlinelibrary.com) DOI 10.1002/jctb.6033

Optimally designed reactive distillation processes for eco-efficient production of ethyl levulinate

José A Vázquez-Castillo,[a] Gabriel Contreras-Zarazúa,[b] Juan G Segovia-Hernández[b] and Anton A Kiss[c,d*]

Abstract

BACKGROUND: Ethyl levulinate (EL) is an important chemical that can be used as a bio-based replacement of fuel additives such as methyl *tert*-butyl ether (MTBE) and *tert*-amyl methyl ether (TAME). EL production from lactic acid and ethanol is a viable option, as both precursors can be obtained from biomass. However, the problem of EL production by esterification is that this reaction is hindered by the chemical equilibrium limitations and the boiling points ranking, which is not the most favorable.

RESULTS: This study provides novel optimally designed reactive distillation (RD) processes for the production of EL, taking into account costs, environmental impact and safety. The thermally coupled RD process is the most appealing, with the lowest energy use (1.667 MJ kg^{-1} EL), minimal investment cost, major energy savings (up to 54.3% lower than other RD processes), reduced environmental impact (up to 51% lower ECO99 index value) and similar safety as other RD processes considered (less than 2% differences in the individual risk (IR) indicator).

CONCLUSION: The multi-objective optimization approach used here showed its robustness, practicality and flexibility to provide multiple optimal designs of intensified processes that are economically attractive, environmentally friendly and inherently safe.

Keywords: reactive distillation; sustainable process; optimal design; safety; green chemistry

INTRODUCTION

Levulinic acid (LA) is a key bio-based chemical used among others in the production of eco-friendly herbicides, flavor and fragrance ingredients, skin creams and degreasers. Production of LA is hindered by key challenges such as the low concentrations of LA resulting from the deconstruction of cellulose and recovering the mineral acids used for that task. LA is usually recovered from the reaction mixture using energy-intensive processes involving distillation, (reactive) extraction, adsorption, electrodialysis, esterification and reactive distillation.[1,2]

Promising fuel additives can be obtained from LA, such as 2-methyltetrahydrofuran (MTHF) and ethyl levulinate (EL). The use of biofuel additives grants several advantages, such as better performance of engines and lower environmental impacts. Particularly, EL can be used as a bio-based replacement of fuel additives such as methyl *tert*-butyl ether (MTBE) and *tert*-amyl methyl ether (TAME).[3] The market cost of MTHF and EL is in the range of \$1.53–5.68/L, which is still higher than the price of petrol or additives in many countries.[4] Therefore reducing the production cost of bio-based additives is a stimulating economic reason to optimize their production from LA. The current forecast for EL production is very promising and the global EL market is expected to reach US\$11.8 million by 2022.[5,6] Interest in the development of economically feasible and sustainable processes for EL has increased owing to the potential application of EL in biodegradable polymers such as polyesters, polyurethane and thermoplastics. EL can be also used to produce diphenolic acid (used to replace the bisphenol A that is widely applied in the production of polycarbonate).[7]

Second-generation biorefineries need to focus on sustainable chemical products made using green chemical technologies with high efficiency as well as improved bioprocesses that could convert biomass directly into esters.[8] In this respect, further

---

* Correspondence to: AA Kiss, School of Chemical Engineering and Analytical Science, The University of Manchester, Manchester, UK. E-mail: tony.kiss@manchester.ac.uk

a Faculty of Chemical Sciences, Autonomous University of Chihuahua, Chihuahua, Mexico

b Department of Chemical Engineering, University of Guanajuato, Guanajuato, Mexico

c School of Chemical Engineering and Analytical Science, The University of Manchester, Manchester, UK

d Sustainable Process Technology Group, Faculty of Science and Technology, University of Twente, Enschede, The Netherlands

research into the production of EL is necessary, for example on high-efficiency catalysts[9,10] and novel efficient routes that are economically attractive and ecologically friendly.[11] A mesoporous solid superacidic zirconia-modified catalyst was reported to exhibit high performance for the LA esterification to EL,[12] while others used acid ionic liquid as catalyst to produce EL.[13] Studies also point out some challenges to be addressed for competitive EL bioprocesses, such as the hydrolysis of biomass and the consequent separation operations of products and by-products.[6] The route that involves the direct conversion of lignocellulosic material through the hydrolysis reaction to produce EL presents drawbacks, e.g. energy-demanding difficult separations employing techniques such as vacuum distillation, evaporation, stripping or extraction with harmful toxic solvents. The downstream processing would clearly benefit from more insights into fluid separations.[14]

A more appealing route is the conversion of biomass to LA, followed by esterification with ethanol to obtain EL,[15] but this route is limited by the equilibrium of the reaction.[16] Reactive distillation (RD) can be effectively used to overcome the equilibrium limitations. This well-known process intensification technique offers higher conversion, better selectivity and reduced operational and capital expenditures as compared with classical processes.[17–19] The advantages of RD are attributed to the continuous removal of the products (thus pulling the chemical equilibrium instead of pushing it with an excess of reactant). Recent studies have also highlighted the reductions in energy usage and costs that can be achieved by applying thermal coupling to RD processes, with energy savings and cost reductions in the range of 24–63% and 8–43% respectively.[20–23] The major reductions in energy use and associated CO_2 emissions are due to the thermal coupling that minimizes the remixing phenomena. Hence thermal coupling helps to further improve the advantages of the RD operation, transforming this operation into a more sustainable and eco-friendly process.

This work is the first to present optimally designed RD processes (including thermal coupling) for EL production, taking into account several key aspects for optimization: total annual cost (TAC), environmental impact (Eco-indicator 99) and process safety (individual risk). To allow a fair comparison, some of the topology of the RD processes is based on previous work reported recently (but focused on economics only),[24] while others are new (e.g. based on RD and dividing wall column (DWC) technology). However, besides considering the economic aspects, this work uses rigorous process simulations in Aspen Plus and implements a rigorous multi-objective optimization algorithm in which the three key factors (economic, environmental and safety) are simultaneously evaluated. The meta-heuristic optimization algorithm used here is based on multi-objective differential evolution and tabu list (MODE-TL). This multi-objective algorithm allows the comparison of multiple solutions and was used to determine multiple designs that meet the desired specifications of the products at minimal cost and environmental impact while meeting process safety standards. Obviously, the assessment of the economic, environmental and safety issues has a strong relevance in the context of designing green and sustainable processes for a circular economy.[25,26]

PROBLEM STATEMENT

EL production from LA and ethanol is a viable biofuel option, since both precursors can be obtained from biomass. However, the problem of EL production by esterification is that this reaction is hindered by the chemical equilibrium limitations. RD is a feasible process that could overcome all these limitations,[27] but the boiling points ranking is not the most favorable as the reactants are the lightest and heaviest components respectively, while the products are mid-boiling components – so this system belongs to group I_r[28,29] with the order of normal boiling points: ethanol ($T_{b,A}$ = 78.3 °C), water ($T_{b,C}$ = 100 °C), ethyl levulinate ($T_{b,D}$ = 205.8 °C) and levulinic acid ($T_{b,B}$ = 257.0 °C). The consequence is that a single RD column is insufficient to produce both products on-spec, hence at least two columns will be required for neat operation using stoichiometric reactants ratio (Fig. 1). To solve this problem, this study proposes several optimally designed RD processes that make use of multiple distillation columns that are thermally coupled and/or heat integrated for increased eco-efficiency.

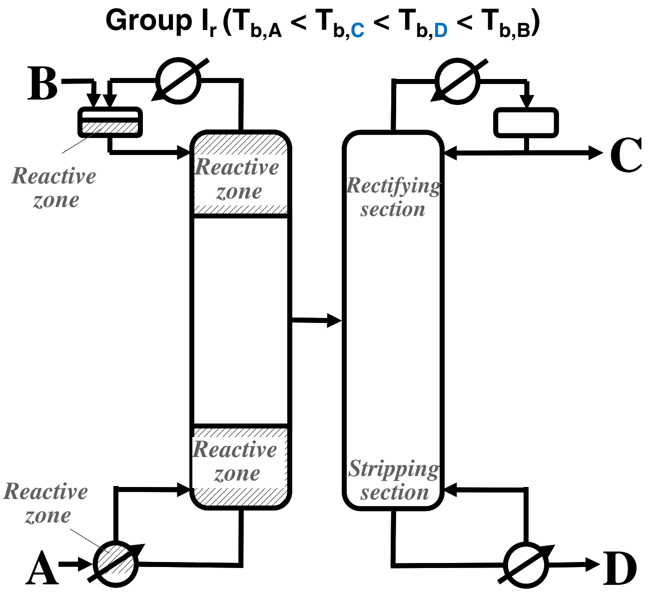

Figure 1. Reactive distillation process for quaternary systems (group I_r).

APPROACH AND METHODOLOGY

The RD process configurations considered in this work are shown in Fig. 2: conventional RD process (CRDP), thermally coupled RD (TCRD), RD with heat integration (RDHI), thermally coupled and heat integrated RD (THRD) and RD with dividing wall column (PDWC). These RD processes produce 100 kmol h^{-1} EL (equivalent to about 120 kt year^{-1}) with a purity of 99.5 mol% (same as for water by-product). This is consistent with the purity values reported in previous studies about the design of EL processes,[6] and in the context of using EL as a fuel bio-additive.[30]

All processes consist of a reactive distillation column (RDC) and two separation columns (RC-1 and RC-2). The fresh reagents (LA and ethanol) are fed near the top of the RDC at a rate of 100 kmol h^{-1} each. An excess of LA is actually used owing to the recycle of unreacted LA (in addition to the continuous reflux of LA). Excess operation was proved to perform better than neat operation.[24] The first separation column (RC-1) performs the separation of water by-product as distillate from the main product (EL) and the unreacted LA. The second separation column (RC-2)

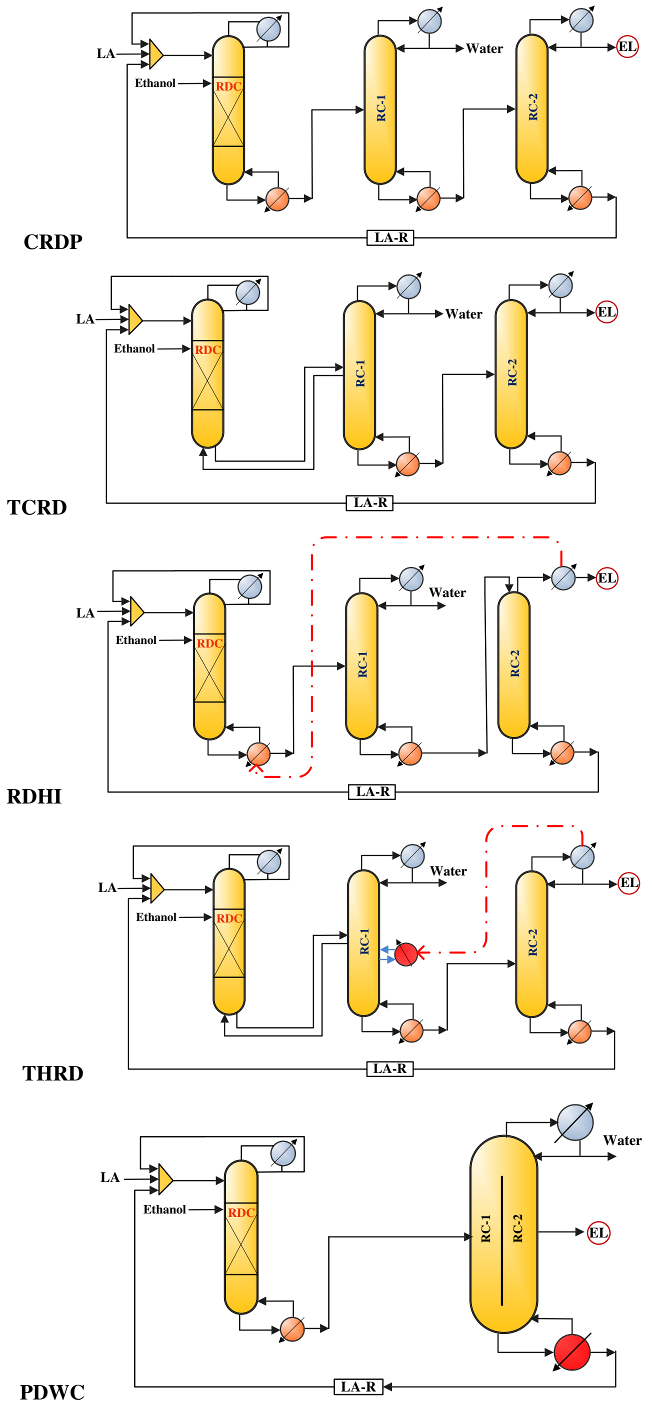

Figure 2. Reactive distillation-based processes to produce ethyl levulinate.

performs the separation of EL product as top distillate from the excess LA that is removed as bottom product and recycled (LA-R) to the RDC unit.

The thermal coupling in TCRD is performed between the reboiler of the RC-1 column and the bottom of the RDC unit, whereas the RDHI configuration uses heat integration between the top vapor leaving the RC-2 column (highest-temperature equipment) and the bottom of the RDC unit. THRD combines thermal coupling (between the reboiler of RC-1 and the bottom part of the RDC unit) and heat integration (between the top vapor of RC-2 and a withdrawal product side-stream of RC-1). PDWC is a novel configuration that includes an RDC and a DWC, which results from merging columns RC-1 and RC-2 in a single shell divided by an internal wall. From a conceptual point of view, the length of the wall is determined by the number of trays of the sections of columns RC-1 and RC-2.

Chemistry and kinetics

EL is produced by the esterification reaction of LA with ethanol, where the following notation is used: A, levulinic acid; B, ethanol; C, ethyl levulinate; D, water.

$$\mathrm{C_5H_8O_3\,(A) + C_2H_5OH\,(B)} \underset{k_2}{\overset{k_1}{\rightleftharpoons}} \mathrm{C_7H_{12}O_3\,(C) + H_2O\,(D)} \tag{1}$$

The reaction rate is given by the kinetic equation

$$-r_\mathrm{A} = k_1\left(a_\mathrm{A}a_\mathrm{B} - a_\mathrm{C}a_\mathrm{D}/K_\mathrm{a}\right) \tag{2}$$

and the equilibrium constant (K_a) can be expressed as the ratio between the kinetic constants of the forward and reverse reactions:

$$K_\mathrm{a} = k_1/k_2 \tag{3}$$

The kinetic constants k_1 and k_2 are expressed as follows:

$$k_1 = A_\mathrm{f}\exp\left(-E_{0,\mathrm{f}}/RT\right) \text{ and } k_2 = A_\mathrm{f}\exp\left(-E_{0,\mathrm{r}}/RT\right) \tag{4}$$

The kinetic parameters of the esterification reaction are the following:[31]

$$A_\mathrm{f}\ \left(\mathrm{mol\,kg^{-1}\,min^{-1}}\right) = 0.08\times10^8 \tag{5}$$

$$E_{0,\mathrm{f}}\ \left(\mathrm{kJ\,kg^{-1}\,min^{-1}}\right) = 37.79 \tag{6}$$

$$A_\mathrm{f}/A_\mathrm{r} = 43.33 \tag{7}$$

$$\Delta h_\mathrm{f}/R\ (\mathrm{K}) = 105.2 \tag{8}$$

Property model

The non-random two-liquid with Hayden–O'Connell correction (NRTL-HOC) model was selected as an adequate thermodynamic model to estimate the vapor–liquid equilibrium (VLE). This property model handles in a consistent way the phenomena associated with the presence of polar compounds and carboxylic acids, such as the solvation and the dimerization in the vapor phase of carboxylic acids.[17,32] The binary interaction parameters of the components were taken from another reported work[33] and implemented in Aspen Plus v8.4.

Process optimization

This study uses a multi-objective meta-heuristic optimization algorithm based on differential evolution and tabu list (MODE-TL), further details of which can be found elsewhere.[34] This algorithm allows the comparison of multiple solutions of optimized designs in the terms of multiple objective functions, described hereafter.

Total annual cost

The total annual cost (TAC) of each reactive distillation process considered here has been estimated as follows:

$$\mathrm{TAC} = \mathrm{OPEX} + \mathrm{CAPEX}/\text{payback period} \tag{9}$$

where OPEX and CAPEX represent operating and capital expenditures respectively. The capital cost of each RD process was calculated using the modular method.[35] The capital cost includes the cost of distillation columns, trays, heat exchangers and compressors. The parameters and equations to calculate the cost can be found elsewhere.[36] Carbon steel was the assumed construction material for all equipment, and a payback time of 5 years was considered. The operating cost includes cooling utilities, heating utilities and 8400 h of yearly operation for each configuration. The utilities considered were oil for heating at \$6.28/GJ, low-pressure steam (6 bar, 160 °C) at \$7.78/GJ, electric power with a cost of \$16.8/GJ and cooling water (received at 20 °C and returned at 30 °C) with a unit cost of \$0.72/GJ.[37,38]

Environmental impact

This was quantified by the Eco-indicator 99 (ECO99). ECO99 was used to evaluate the sustainability of the processes, to quantify the environmental impact and to detect the factors that largely affect the environmental impact. This approach was proposed by Goedkoop and Spriensma.[39] Several authors have demonstrated that applying ECO99 during the design and synthesis phases of chemical processes can lead to significant improvements and waste reduction.[40–42] This methodology is consistent with the philosophy of life cycle analysis (LCA) and sustainability in the design of chemical processes. The calculation of ECO99 is based on evaluating three major damage categories: human health, ecosystem quality and resources depletion. Each category is divided into 11 sub-categories. In the case of distillation columns, the factors that have the strongest influence on ECO99 are the steam used to supply the heat duty, the electricity utilized for pumping of cooling water and the steel necessary to build the equipment. ECO 99 is defined as

$$\text{Eco} - \text{Indicator}\ \ 99 = \sum_{b} \sum_{d} \sum_{k \in K} \delta_d \omega_d \beta_b \alpha_{b,k} \tag{10}$$

where β_b represents the total amount of chemical b released per unit of reference flow due to direct emissions, $\alpha_{b,k}$ is the damage caused in category k per unit of chemical b released to the environment, ω_d is a weighting factor for damage in category d, and δ_d is a normalization factor for damage of category d. According to the importance of three major impact categories (human health, ecosystem quality and resources depletion), the weighting for ECO99 was specified as follows: damage to human health and damage to ecosystem quality were set equal in importance (i.e. both categories were equally weighted), while damage to resources was considered to be half of importance for weighting. The impact categories and the values of these used in this study were taken from a previously reported work.[32] The scale of the values was chosen such that the value of 1 point is representative for a 1000th of the yearly environmental load of one average EU inhabitant.

Process safety

This was quantified by the individual risk (IR) index. The IR can be defined as the risk of injury or death to a person in the vicinity of a hazard.[43,44] The main objective of this index is the estimation of likelihood affectation caused by a specific incident that occurs with a certain frequency. The IR does not depend on the number of people exposed. The mathematical expression for calculating the individual risk is

$$\mathrm{IR} = \sum f_i P_{x.y} \tag{11}$$

where f_i is the occurrence frequency of incident i, and $P_{x,y}$ is the probability of injury or death caused by incident i. In this work, an irreversible injury (death) is used, for which more data are recorded. The calculation of IR can be carried out through quantitative risk analysis (QRA), which is a methodology used to identify incidents and accidents and their consequences. QRA starts with the identification of possible incidents, which for distillation columns are identified as continuous and instantaneous releases. A continuous release is produced mainly by a rupture in a pipeline or a partial rupture on a process vessel causing a leak. An instantaneous release consists in the total loss of matter from the process equipment originated by a catastrophic rupture of the vessel. These incidents were determined through a hazard and operability (HAZOP) study. The frequencies for each incident (f_i) were taken according to the values previously reported by the American Institute of Chemical Engineers (AIChE)[43] and using the event tree diagrams obtained with all probabilities of instantaneous and continuous incidents, along with their respective frequencies. Accordingly, instantaneous incidents are boiling liquid expanding vapor explosion (BLEVE), unconfined vapor cloud explosion (UVCE), flash fire and toxic release, whereas continuous release incidents are jet fire, flash fire and toxic release.

Once the incidents have been identified, the probability $P_{x,y}$ can be calculated through a consequence assessment, which consists in determining the physical variables such as the thermal radiation, the overpressure and the concentration of the leak originated by incidents, and their respective damages. The calculation of the physical variables was realized according to the equations reported by the AIChE[43] and some other authors.[45,46] The worst scenario was considered for calculating the dispersion, as well as a wind speed of 1.5 m s^{-1} and atmospheric stability type F.[43,45,46]

The quantification of the damage caused by physical variables of each incident is calculated through a vulnerability model commonly known as the probit model. In this work, the damage considered is death due to fires, explosions and toxic releases. The probit models associated with deaths by thermal radiation ($t_e E_r$) and overpressure due to explosions ($p°$) are

$$Y = -14.9 + 2.56 \ln \left(t_{\mathrm{e}} E_{\mathrm{r}}^{4/3} / 10^4 \right) \tag{12}$$

$$Y = -77.1 + 6.91 \ln \left(p^{\mathrm{o}} \right) \tag{13}$$

Owing to the lack of reported probit models of toxicity of components considered in this work, the calculation of the damage for toxic releases was carried out using the median lethal concentration (LC50).[43] Finally, the probability $P_{x,y}$ is calculated by substituting the probit results into the following equation:

$$Px, y = 0.5 \left\{ 1 + \operatorname{erf} \left[(Y - 5) / \sqrt{2} \right] \right\} \tag{14}$$

The physical properties for each substance used for the consequence assessment are reported in Table 1. These were taken from the National Institute for Occupational Safety and Health.[47]

Table 1. Safety-related physical properties of components

Component	Lower flammability limit (LFL)	Upper flammability limit (UFL)	Median lethal concentration (LC50) (ppm L^{-1} h^{-1})	Heat of combustion (kJ mol^{-1})
Ethanol	3.3	19	14 000	2344
Levulinic acid	1.8	9.87	1500	726
Ethyl levulinate	1.8	9.89	83	876.1

Table 2. Discrete and continuous decision variables for optimized RD processes

	CRDP		TCRD		RDHI		THRD		PDWC	
Decision variable	Cont.	Disc.	Cont.	Disc.	Disc.	Disc.	Cont.	Disc.	Cont.	Disc.
Number of stages, RDC		X		X	X	X		X		X
Number of reactive stages		X		X	X	X		X		X
Heat duty of RDC, kW	X								X	
Distillate flow, kmol h^{-1}	X		X				X		X	
Diameter of RDC, m	X		X				X		X	
Number of stages, RC-1		X		X	X	X		X		X
Feed stage, RC-1		X		X	X	X		X		X
Reflux ratio of RC-1	X		X				X			
Interlinking flow, kmol h^{-1}			X				X		X	
Bottom flow of RC-1, kmol h^{-1}	X		X				X			
Diameter of RC-1, m	X		X				X		X	
Withdrawal side stage					X	X		X		
Side flow, kmol h^{-1}							X			
Number of stages, RC-2		X		X	X	X		X		X
Feed stage, RC-2		X		X	X	X		X		X
Reflux ratio of RC-2							X		X	
Bottom flow, kmol h^{-1}	X		X						X	
Heat duty of RC-2, kW	X		X				X		X	
Diameter of RC-2, m	X		X						X	
Total number of variables	15		15		13		17		16	

Objective function

The optimal design of RD processes means minimizing the objective function that considers TAC, ECO99 and IR. These are restricted to satisfy the mass flow rate and purity constraints. All objectives (TAC, ECO99, IR) have been considered equally important, thus the weights are the same:

$$\min\,[\mathrm{TAC}, \mathrm{ECO99}, \mathrm{IR}] = f\left(NS_i, Fs_i, R_i, VF, LF, DC_i, HD_i, k, C_{i,j}\right) \quad (15)$$

subject to

$$\mathbf{y}_m \geq \mathbf{x}_m \text{ and } \mathbf{w}_m \geq \mathbf{u}_m \quad (16)$$

where NS_i is the total number of stages, Fs_i are the feed stages, R_i the reflux ratios, VF and LF the interconnection vapor and liquid flows respectively, DC_i the distillation column diameters, HD_i the heat duties of the reboilers and $C_{i,j}$ the concentrations of chemicals inside the column. The optimization problem is subjected to constraints related to purity and mass flow rate. In this work, $\mathbf{y}_m$ and $\mathbf{w}_m$ are the vectors of obtained purity and mass flow rate and $\mathbf{u}_m$ and $\mathbf{x}_m$ are the vectors of required purity and mass flow rate respectively. The purity constraints for EL and water were defined as 99.5 mol%, while the molar flow rate was at least 99.5 kmol h^{-1} for both EL and water in their respective streams. The decision variables used for optimizing the RD processes (Fig. 2) are a combination of discrete and continuous variables, all of them conveniently listed in Table 2.

Multi-objective optimization strategy

The multi-objective optimization algorithm (MODE-TL) used in this work is a powerful stochastic global optimization tool which combines two optimization techniques: differential evolution (DE) and tabu search (TS). The combination of the features of these techniques confers on the multi-objective optimization algorithm a faster convergence to global optima when compared with a single DE method, and less computational time and effort. A more extensive description of the differential evolution with tabu list (DETL) algorithm is provided by other authors,[34,48] as well as in our recent study.[46]

The values of the parameters associated with the used MODE-TL algorithm are the following: population size (NP), 200 individuals; generations number (GenMax), 500; tabu list size (TLS), 100 individuals; tabu radius (TR), 0.01; crossover fractions (Cr), 0.8; mutation fractions (F), 0.3. The values of NP, GenMax and TLS were determined through a previous tuning process on the optimization algorithm, whereas the values of Cr, TR and F were taken from the recommended values for these parameters.[34,48] This optimization method had been implemented using a hybrid platform that interconnects Aspen Plus and Excel through Visual Basic. Rigorous simulations are implemented in Aspen Plus using the RADFRAC model that includes all mass and energy balances, equilibrium and reaction (MESHR) equations. Recent implementations of this algorithm for the optimization of multiple chemical processes can be

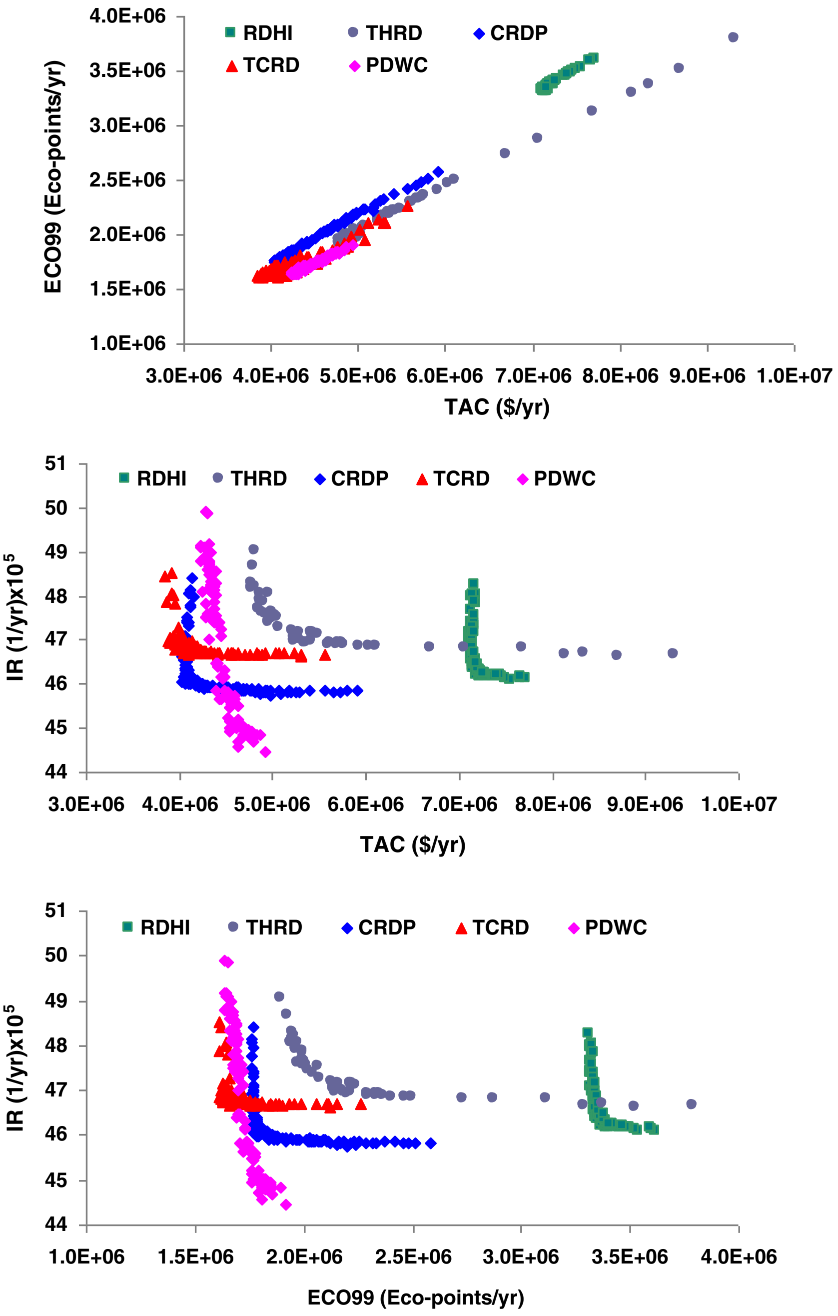

Figure 3. Pareto fronts for TAC *vs* ECO99, TAC *vs* IR and ECO99 *vs* IR.

found in other works that proved its robustness, practicality and flexibility to provide the multiple designs of these processes.[49,50]

RESULTS AND DISCUSSION

This section provides the simulation results of the optimized RD processes considering the economic, environmental and safety indices. All processes were rigorously modeled using the process simulator Aspen Plus v8.4 (including the RADFRAC module) that provided the complete set of mass and energy balances along with the phase equilibrium calculations. All the runs to carry out the optimization were performed on an Intel® Core™ i7-4790 CPU @ 3.6 GHz, 12 GB computer.

Pareto charts are used in order to simplify the analysis of the results in a practical way. These Pareto fronts correspond to the 200 individuals for the generation 500, which is the last generation. By the generation 500, there are no more significant improvements to all objective functions. The Pareto fronts are studied according to utopic point methodology that is based on the Pareto optimality concept. A Pareto optimal is a set of solutions on the border of the feasible solutions (usually called a Pareto front), and the utopic point corresponds to the solution were two or more objectives are in equilibrium and these objectives cannot improve anymore.[51]

The solutions in the Pareto chart can help in the decision-making process by selecting the best option among all of the configurations to produce EL. The Pareto charts obtained for all of the RD processes at the end of the optimization process are illustrated in Fig. 3 (lower left corner is better). Each point in the graphics represents a solution or design that meets the purity

Table 3. Design variables of optimal designs of RD processes

Design variable	CRDP	TCRD	RDHI	THRD	PDWC
Topology of columns					
Number of stages, RDC	83	93	48	58	66
Number of reactive stages, RDC	2–45	2–63	2–23	2–37	2–32
Number of stages, RC-1	26	23	32	19	43
Number of stages, RC-2	31	34	16	16	57
Feed stage, RC-1	13	15	21	15	–
Feed stage, RC-2	21	27	1	14	18
Withdrawal side stage, RC-1	–	–	–	14	–
Withdrawal side stage, RC-2	–	–	–	–	22
Diameter of RDC, m	1.009	1.334	1.04	1.17	1.20
Diameter of RC-1, m	1.170	1.036	1.13	1.60	–
Diameter of RC-2, m	1.080	1.090	1.07	1.88	1.56
Operating conditions					
Top pressure, atm	1	1	1	1	1
Distillate flow, kmol h^{-1}	493.73	441.58	532.464	342.606	201.294
Tray holdup, L	44.004	76.951	46.687	59.442	62.259
Reflux ratio of RC-1	0.5371	0.5819	0.9651	1.152	–
Reflux ratio of RC-2	–	–	–	0.7045	2.27
Heat duty of RDC, kW	3019.17	0	10 211.3	0	2630.71
Heat duty of RC-1, kW	2738.91	4830.74	3226.57	6750.52	–
Heat duty of RC-2, kW	1698.80	1839.34	1122.45	2052.30	4745.72
Interlinking flow, kmol h^{-1}	–	151.446	–	272.922	127.879
Side flow of RC-2, kmol h^{-1}	–	–	–	24.7091	100.368
Bottom flow of RC-1, kmol h^{-1}	118.687	119.813	117.416	125.435	–
Bottom flow of RC-2, kmol h^{-1}	18.7575	19.9172	17.4219	25.6693	34.7812
Temperature bottom, RDC (°C)	118.95	117.70	117.94	117.15	122.72
Temperature bottom, RC-1 (°C)	227.31	232.07	227.47	228.63	–
Temperature bottom, RC-2 (°C)	247.83	267.91	230.42	235.69	278.02
Molar flow rates of process streams					
Ethyl levulinate stream, kmol h^{-1}	99.5081	99.877	99.5036	99.7631	99.9950
Water stream, kmol h^{-1}	99.6249	99.990	99.5128	99.9929	99.6316
Purity of products (molar fraction)					
Ethyl levulinate	0.9964	0.9998	0.9951	0.9999	0.9962
Water	0.9957	0.9981	0.9950	0.9979	0.9999
Performance indices					
Energy per ton of product (GJ ton^{-1} EL)	1.8712	1.6676	3.6539	2.2033	1.8420
Total CO_2 emissions (kt $year^{-1}$)	14.960	13.309	29.707	17.650	14.107
CO_2 emissions (kg ton^{-1} EL)	124.14	110.04	246.53	146.09	116.49
Utilities cost (million \$/yr)	3.8125	3.7141	6.9426	5.0005	4.2692
Equipment cost (million \$)	0.2544	0.2305	0.2767	0.2218	0.2580
TAC (million \$/yr)	4.0670	3.9447	7.2193	5.2224	4.5272
ECO99 (million Eco-points/yr)	1.7803	1.6592	3.3916	2.1465	1.7606
IR (1/yr) $\times 10^5$	45.994	46.766	46.150	46.962	44.934

requirements with the best values of the three objective functions under evaluation.

The shapes of Pareto fronts for ECO99 *vs* TAC are similar for all process configurations. This is explained by the influence of the total energy used in each process (e.g. the energy required in the form of steam for heating, the electricity used for pumping of cooling water, the amount of steel required to build the equipment). The results are consistent with the findings reported for other processes involving separation operations.[52] Important reductions in the ECO99 values for the TCRD process are obtained due to the energy savings of this process with respect to the others. This work also reveals that the PDWC configuration is actually not the best alternative in terms of energy savings and TAC, as one might have expected, since the integration of RC-1 and RC-2 columns in a single shell leads to an increased column diameter and larger amounts of substances present and processed in the column, thus leading to an increase in the energy use and TAC.

Concerning the Pareto front of IR *vs* TAC, it can be noticed that the forms exhibit a trend of opposite objectives. This behavior indicates that the selection of a design with the lowest TAC causes the IR to increase, hence the solutions that offer the best trade-offs between the two objectives are those located in the curve zone of the Pareto chart. Two key factors determine the value of the IR index in the processes: one of them is represented by the physical properties of the substances and the other is the amount of the substances inside the columns. For instance, it was found here that

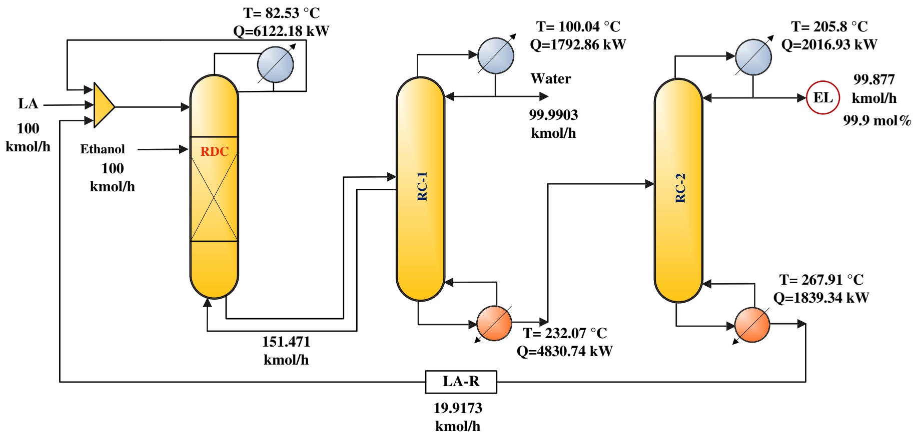

Figure 4. Molar flows, temperatures and energy requirements for optimal TCRD process.

there is a direct trade-off among the diameter of the RDC and the diameters of the separation columns. Despite a large value of diameter of RDC in a process with low values of diameters of both RC-1 and RC-2, the process will be favored in the IR index, meaning that the process will be safer than a process with larger diameters in RC-1 and RC-2.

The Pareto front of IR *vs* ECO99 for all processes exhibits a similar trend as the IR *vs* TAC Pareto for these same configurations. In the optimal designs, the larger the reflux ratios and reboiler duties, the higher is the usage of heating services and electricity for cooling services, and these larger values have a direct contribution in the increment of the ECO99 values.

According to the behavior of the Paretos of the objective functions IR *vs* ECO99 and IR *vs* TAC, it is possible to assert that the best optimal designs of all processes are found in the zone of the Pareto that compensates both objectives, this being the curve zone. Therefore, with the selection of a design that compensates the IR index with TAC, this choice directly balances the IR index with ECO99.

The chosen designs were selected according to the utopian point methodology, in which the utopic point corresponds to a hypothetical and ideal solution on the border of the Pareto front where two objectives cannot improve anymore and both are in equilibrium. The selected designs correspond to solutions closer to the utopic point.[51] The practicality of this methodology has been proved in recent work by other authors.[46,49,50]

Table 3 provides the design variables of the selected designs of the Pareto charts for all RD processes – the points selected for the sequences are the ones located in the curve zone where the best trade-offs between the two objectives are established. The TCRD process revealed the lowest energy use (10.8% lower than CRDP, 24.3% lower than THRD, 54.3% lower than RDHI and 9.6% lower than PDWC). The energy savings are also reflected in the value of TAC for TCRD, which is 3.1, 24.4, 45.3 and 12.8% lower as compared with CRDP, THRD, RDHI and PDWC respectively. In terms of environmental impact (ECO99), TCRD presents a value that is 6.8, 22.7,51.0 and 5.7% lower as compared with CRDP, THRD, RDHI and PDWC respectively. However, in terms of safety, all processes are rather similar, with small differences in the IR index of 2% or less. Yet, these small differences in IR are translated into valuable information on the probability of catastrophic events in the process, because of the models utilized in the calculation of the IR index, so even a difference of 1% in the IR value of a process compared with others implies differences of tens or even hundreds of meters in the affected region caused by events such as explosions, fires and instantaneous releases.

The results obtained in this work are different than reports of other authors.[24] The contrasts are explained by the fact that the implementation of a multi-objective optimization algorithm needs some adjustments to the rigorous process simulation. For example, for the THRD process, the withdrawal side stage number and the side molar flow rate in the first separation column are both variables subject to optimization, while an additional constraint was added for the minimum temperature difference (driving force of 10 K) as it was found that only a fraction of the condenser energy of RC-2 was feasible to be utilized. In the case of the RDHI sequence, a liquid stream enters the top of the RC-2 column while a vapor stream leaves the top via a heat exchanger, the heat duty of which is the heat that is subtracted from the heat duty of the reboiler of the reactive column. Based on the overall comparison, the TCRD process is the most appealing to be implemented in EL production, having the lowest specific energy requirement (1.667 MJ kg^{-1} EL) and an annual cost of utilities of only \$30.35 per ton of EL produced, as well as lowest CO_2 emissions (110.4 kg ton^{-1} EL) due to thermal coupling. Figure 4 provides the molar flow rates, temperatures and energy use for the optimal TCRD process.

CONCLUSIONS

The simulation results show that the eco-efficient production of EL is possible in RD processes with thermal coupling and/or heat integration. The multi-objective optimization takes into account simultaneously the total annual cost (TAC), Eco-indicator 99 (ECO99) and individual risk (IR), these parameters being selected according to the principles of green sustainable processes and circular economy, as they provide good detailed metrics to measure the economy, environmental impact and safety of the process, which are necessary to create a sustainable process.

The results of the optimization revealed that the TCRD process has the lowest energy use (1.667 MJ kg^{-1} EL), with major energy savings (9.6–54.3% lower than other RD processes), reduced environmental impact (5.7–51% lower ECO99 index value) and similar process safety (less than 2% difference as compared with other RD processes considered). Thus the TCRD process is suggested as the best process alternative to produce EL, although there is room for further selection of other feasible RD processes where other trade-offs among the indicators may be devised. The multi-objective optimization approach used here showed its robustness, practicality and flexibility to provide multiple designs of intensified processes that are economically attractive, environmentally friendly and inherently safe.

A potential way to further improve the EL production could be the use of RD starting from an aqueous solution of LA (instead of pure LA) that undergoes esterification with alcohols, but this is a topic for a future research study.

ACKNOWLEDGEMENTS

JAV-C acknowledges the financial support provided by a PRODEP-SEP grant. AAK gratefully acknowledges the Royal Society Wolfson Research Merit Award. The authors also thank the reviewers for their insightful comments and suggestions.

REFERENCES

1 Joglekar HG, Rahman I, Babu S, Kulkarni BD and Joshi A, Comparative assessment of downstream processing options for lactic acid. *Sep Purif Technol* **52**:1–17 (2006).

2 Komesu A, Wolf Maciel MR, de Oliveira JAR, da Silva Martins LH and Maciel Filho R, Purification of lactic acid produced by fermentation: focus on non-traditional distillation processes. *Sep Purif Rev* **46**:241–254 (2017).

3 Shrivastav G, Khan TS, Agarwal M and Haider MA, Reformulation of gasoline to replace aromatics by biomass-derived alkyl levulinates. *ACS Sustain Chem Eng* **5**:7118–7127 (2017).

4 Gunukula S, Pendse HP, DeSisto WJ and Wheeler MC, Heuristics to guide the development of sustainable, biomass-derived, platform chemical derivatives. *ACS Sustain Chem Eng* **6**:5533–5539 (2018).

5 Grand View Research, *Ethyl Levulinate Market Worth $11.8 Million by 2022*. (2016). Available: http://www.grandviewresearch.com/press-release/global-ethyl-levulinate-market [23 September 2018].

6 Leal Silva JF, Grekin R, Mariano AP and Maciel Filho R, Making levulinic acid and ethyl levulinate economically viable: a worldwide technoeconomic and environmental assessment of possible routes. *Energy Technol* **6**:613–639 (2018).

7 Isikgor FH and Becer CR, Lignocellulosic biomass: a sustainable platform for the production of bio-based chemicals and polymers. *Polym Chem* **6**:4497–4559 (2015).

8 Clark JH, Green chemistry for the second generation biorefinery – sustainable chemical manufacturing based on biomass. *J Chem Technol Biotechnol* **82**:603–609 (2007).

9 Zhang J, Wu SB, Li B and Zhang HD, Advances in the catalytic production of valuable levulinic acid derivatives. *ChemCatChem* **4**:1230–1237 (2012).

10 Nandiwale KY, Niphadkar PS, Deshpande SS and Bokade VV, Esterification of renewable levulinic acid to ethyl levulinate biodiesel catalyzed by highly active and reusable desilicated H-ZSM-5. *J Chem Technol Biotechnol* **89**:1507–1515 (2014).

11 Démolis A, Essayem N and Rataboul F, Synthesis and applications of alkyl levulinates. *ACS Sustain Chem Eng* **2**:1338–1352 (2014).

12 Yadav GD and Yadav AR, Synthesis of ethyl levulinate as fuel additives using heterogeneous solid superacidic catalysts: efficacy and kinetic modeling. *Chem Eng J* **243**:556–563 (2014).

13 Ramli NAS and Amin NAS, Optimization of biomass conversion to levulinic acid in acidic ionic liquid and upgrading of levulinic acid to ethyl levulinate. *BioEnergy Res* **10**:50–63 (2017).

14 Blahušiak M, Kiss AA, Babic K, Kersten SRA, Bargeman G and Schuur B, Insights into the selection and design of fluid separation processes. *Sep Purif Technol* **194**:301–318 (2018).

15 Fernandes DR, Rocha AS, Mai EF, Mota CJA and da Silva VT, Levulinic acid esterification with ethanol to ethyl levulinate production over solid acid catalysts. *Appl Catal A* **425–426**:199–204 (2012).

16 Dai J, Peng L and Li H, Intensified ethyl levulinate production from cellulose using a combination of low loading H_2SO_4 and $Al(OTf)_3$. *Catal Commun* **103**:116–119 (2018).

17 Schmidt-Traub H and Górak A, *Integrated Reaction and Separation Operations*. Springer, Berlin (2006).

18 Kiss AA and Bildea CS, A review on biodiesel production by integrated reactive separation technologies. *J Chem Technol Biotechnol* **87**:861–879 (2012).

19 Kiss AA, *Advanced Distillation Technologies - Design, Control and Applications*. Wiley, Chichester (2013).

20 Cheng K, Wang S-J and Wong DSH, Steady-state design of thermally coupled reactive distillation process for the synthesis of diphenyl carbonate. *Comput Chem Eng* **52**:262–271 (2013).

21 Harvianto GR, Ahmad F and Lee M, A thermally coupled reactive distillation and pervaporation hybrid process for *n*-butyl acetate production with enhanced energy efficiency. *Chem Eng Res Des* **124**:98–113 (2017).

22 Zhang Q, Guo T, Yu C and Li Y, Design and control of different pressure thermally coupled reactive distillation for amyl acetate synthesis. *Chem Eng Process* **121**:170–179 (2017).

23 Zhao T, Li J, Zhou H, Ma Z and Sun L, A thermally coupled reactive distillation process to intensify the synthesis of isopropyl acetate. *Chem Eng Process* **124**:97–108 (2018).

24 Novita FJ, Lee H-Y and Lee M, Energy-efficient design of an ethyl levulinate reactive distillation process via a thermally coupled distillation with external heat integration arrangement. *Ind Eng Chem Res* **56**:7037–7048 (2017).

25 Jiménez-González C and Constable DJC, *Green Chemistry and Engineering. A Practical Design Approach*. Wiley, Hoboken, NJ (2011).

26 Geissdoerfer M, Savaget P, Bocken NMP and Hultink EJ, The Circular Economy – a new sustainability paradigm? *J Clean Prod* **143**:757–768 (2017).

27 Shah M, Kiss AA, Zondervan E and de Haan AB, A systematic framework for the feasibility and technical evaluation of reactive distillation processes. *Chem Eng Process* **60**:55–64 (2012).

28 Muthia R, van der Ham AGJ, Jobson M and Kiss AA, Effect of boiling point rankings and feed locations on the applicability of reactive distillation to quaternary systems. *Chem Eng Res Des* **145**:184–193 (2019).

29 Kiss AA, Process intensification by reactive distillation, in *Process Synthesis and Process Intensification. Methodological Approaches*, ed. by Rong B-G. De Gruyter, Boston, MA, pp. 143–181 2017.

30 Ghosh MK, Howard MS, Zhang Y, Djebbi K, Capriolo G, Farooq A *et al.*, The combustion kinetics of the lignocellulosic biofuel, ethyl levulinate. *Combust Flame* **193**:157–169 (2018).

31 Tsai CY, Kinetic behavior study on the synthesis of ethyl levulinate over heterogeneous catalyst. Master thesis, National Taiwan University of Science and Technology, Teipei (2014).

32 Chaves IDG, López JRG, Zapata JLG, Robayo AL and Niño GR, *Process Analysis and Simulation in Chemical Engineering*. Springer, Cham (2016).

33 Resk AJ, Peereboom L, Kolah AK, Miller DJ and Lira CT, Phase equilibria in systems with levulinic acid and ethyl levulinate. *J Chem Eng Data* **59**:1062–1068 (2014).

34 Sharma S and Rangaiah GP, A hybrid multi-objective optimization algorithm. *5th Int. Symp. on Design, Operation, and Control of Chemical Processes*, pp. 1494–1503 (2010).

35 Ulrich GD, *A Guide to Chemical Engineering Process Design and Economics*. Wiley, New York, NY (1984).

36 Turton R, Bailie RC, Whiting WB and Shaeiwitz JA, *Analysis, Synthesis, and Design of Chemical Processes*. Pearson Education, Upper Saddle River, NJ, USA (2008).

37 Luyben WL, *Principles and Case Studies of Simultaneous Design*. Wiley, Hoboken, NJ (2012).

38 Dimian AC, Bildea CS and Kiss AA, *Integrated Design and Simulation of Chemical Processes*, 2nd edn. Elsevier, Amsterdam (2014).

39 Goedkoop M and Spriensma R, *The Eco-indicator 99. A Damage Oriented Method for Life Cycle Impact Assessment. Methodology Report*. PRé Consultants, Amersfoort (2000).

40 Guillén-Gosálbez G, Caballero JA and Jiménez L, Application of Life Cycle Assessment to the structural optimization of process flowsheets. *Ind Eng Chem Res* **47**:777–789 (2008).

41 Alexander B, Barton G, Petrie J and Romagnoli J, Process synthesis and optimisation tools for environmental design: methodology and structure. *Comput Chem Eng* **24**:1195–1200 (2000).

42 Quiroz-Ramírez JJ, Sánchez-Ramírez E, Hernández-Castro S, Segovia-Hernández JG and Ponce-Ortega JM, Optimal planning of feedstock for butanol production considering economic and environmental aspects. *ACS Sustain Chem Eng* **5**:4018–4030 (2017).

43 American Institute of Chemical Engineers (Center for Chemical Process Safety), *Guidelines for Chemical Process Quantitative Risk Analysis*. John Wiley & Sons, USA (2000).

44 Uijt de Haag PAM and Ale BJM, *Guidelines for Quantitative Risk Assessment*. CPR 18E, Publication Series on Dangerous Substances (PGS 3), Ministerie van Volkshuisvesting, Ruimtelijke Ordening en Milieu, The Netherlands (2005).

45 Medina-Herrera N, Jiménez-Gutiérrez A and Mannan MS, Development of inherently safer distillation systems. *J Loss Prevent Process Ind* **29**:225–239 (2014).

46 Contreras-Zarazúa G, Sánchez-Ramírez E, Vázquez-Castillo JA, Ponce-Ortega JM, Errico M, Kiss AA *et al.*, Inherently safer design and optimization of intensified separation processes for furfural production. *Ind Eng Chem Res* **58**:6105–6120 (2019).

47 National Institute for Occupational Safety and Health (NIOSH), Available: https://www.cdc.gov/niosh/index.htm [23 September 2018].

48 Rangaiah GP ed, *Stochastic Global Optimization. Techniques and Applications in Chemical Engineering*. World Scientific, USA (2010).

49 Contreras-Zarazúa G, Vázquez-Castillo JA, Ramírez-Márquez C, Segovia-Hernández JG and Alcántara-Ávila JR, Multi-objective optimization involving cost and control properties in reactive distillation processes to produce diphenyl carbonate. *Comput Chem Eng* **105**:185–196 (2017).

50 Sánchez-Ramírez E, Quiroz-Ramírez JJ, Hernández S, Segovia-Hernández JG and Kiss AA, Optimal hybrid separations for intensified downstream processing of biobutanol. *Sep Purif Technol* **185**:149–159 (2017).

51 Wang Z and Rangaiah GP, Application and analysis of methods for selecting an optimal solution from the Pareto-optimal front obtained by multiobjective optimization. *Ind Eng Chem Res* **56**:560–574 (2017).

52 Sánchez-Ramírez E, Quiroz-Ramírez JJ, Segovia-Hernández JG, Hernández S and Ponce-Ortega JM, Economic and environmental optimization of the biobutanol purification process. *Clean Technol Environ Pol* **18**:395–411 (2016).

Journal of Chemical Technology & Biotechnology published by John Wiley & Sons Ltd on behalf of Society of Chemical Industry.